

Purification of $\text{Cd}_{1-x}\text{Zn}_x\text{Te}$ crystals from Te inclusions by hot zone method

*S.Solodin, S.Dremlyuzhenko, M.Kolisnik,
A.Kanak, A.Rarenko, Z.Zakharuk, P.Fochuk*

Yu. Fedkovych Chernivtsi National University,
2 Kotziubynskoho Str., 58012 Chernivtsi, Ukraine

Received December 27, 2019

In order to eliminate the Te inclusions in $\text{Cd}_{0.9}\text{Zn}_{0.1}\text{Te}$ crystals grown with the tellurium excess, a hot zone method was used, similar to the traveling heater method, but without additionally weighted tellurium. After such heat treatment, a significant decrease of the density of secondary-phase inclusions was observed. Based on the studies of the Hall constant temperature dependence, a decrease in the concentration of shallow A_1 ($\epsilon_A = 0.03$ eV) and deeper A_2 acceptors ($\epsilon_A = 0.15$ eV) was found; as well, a decrease in the magnitude of the absorption coefficient in the visible and infrared regions of the spectrum was noticed. The concentration of ionized centers was reduced by almost an order of magnitude; this indicates a significant increase of the material purity.

Keywords: Crystals, purification technology, tellurium inclusions, impurity concentration, acceptors.

Очищення кристалів $\text{Cd}_{1-x}\text{Zn}_x\text{Te}$ від вкраплень Te методом гарячої зони.

С.В.Солодін, С.Г.Дремлюженко, М.Г.Колісник, А.І.Канак, Г.І.Раренко, З.І.Захарук, П.М.Фочук

Для усунення вкраплень Te у кристалах $\text{Cd}_{0.9}\text{Zn}_{0.1}\text{Te}$, вирощених із надлишком телуру, застосовано метод гарячої зони, схожий до методу рухомого нагрівача, але без додаткової наважки Te. Після такої термообробки зафіксовано значне зменшення густини вкраплень другої фази. На основі досліджень температурної залежності коефіцієнта Холла виявлено зменшення концентрації мілких A_1 ($\epsilon_A = 0,03$ eВ) та глибших акцепторів A_2 ($\epsilon_A = 0,15$ eВ), а також зменшення величини коефіцієнта поглинання у видимій та інфрачервоній областях спектра. Концентрація іонізованих центрів зменшилася майже на порядок, що вказує на суттєве підвищення чистоти матеріалу.

Для устранения вкраплений Te в кристаллах $\text{Cd}_{0.9}\text{Zn}_{0.1}\text{Te}$, выращенных с избытком теллура, применен метод горячей зоны, похожий на метод подвижного нагревателя, но без дополнительной навески Te. После такой термообработки зафиксировано значительное уменьшение плотности вкраплений второй фазы. На основе исследований температурной зависимости коэффициента Холла выявлено уменьшение концентрации мелких A_1 ($\epsilon_A = 0,03$ эВ) и более глубоких акцепторов A_2 ($\epsilon_A = 0,15$ эВ), а также уменьшения величины коэффициента поглощения в видимой и инфракрасной областях спектра. Концентрация ионизированных центров уменьшилась почти на порядок, что указывает на существенное повышение чистоты материала.

1. Introduction

The $\text{Cd}_{1-x}\text{Zn}_x\text{Te}$ (CZT) solid solution is one of the leading semiconductor materials

for the production of X- and gamma-ray detectors. Despite the well-developed technology for growing CZT crystals [1–5], obtaining a semiconductor material with a

minimal amount of defects remains the actual theme for researches. One of the most widespread defects during the growth of CZT crystals is Te inclusions, caused by the retrograde solubility of tellurium and capture of melt drops, enriched by Te, during the solid phase crystallization [6]. The presence of Te inclusions affects the optical and electrical characteristics of the material, reducing the performance of detectors, diminishing the mobility of carriers and charge collection efficiency [7–9]. For complete elimination or reduction of the size and the number of secondary-phase inclusions in the CZT matrix, a post-growth heat treatment (annealing) of crystals is used [10–12]. Such treatment is usually carried out in the atmosphere of both Cd and Te vapors [13, 14]. However, the elimination of bulk Te inclusions by such methods results in the appearance of interstitial atoms and anti-structural defects, as well as a possible change in stoichiometry, which complicates the use of these crystals as detectors [15]. In papers [16, 17], it is shown, that in the CdTe and $Cd_{1-x}Mn_xTe$ crystals it is possible to eliminate the Te inclusions, avoiding these disadvantages, if a modified traveling heater method is used, but without an additionally weighted tellurium (hereinafter — method of purification by the hot zone (MPHZ)). The hot zone temperature must be higher than the Te melting temperature, but lower than the matrix one. The rate of zone movement along the crystal is very slow (0.6 mm/day). Molten Te inclusions travel together with the zone and, at the end of the process, they were brought to the surface of the ingot. Herewith, the stoichiometry of the material does not change and its electro-physical parameters are improved. The advantage of the MPHZ is that Te inclusions enriched by uncontrolled impurities simultaneously move to the surface of the ingot, thus the crystal is purified from these impurities.

In this paper, we evaluated the MPHZ efficiency to eliminate the Te inclusions in CZT crystals.

2. Experimental

For the research, two $Cd_{0.9}Zn_{0.1}Te$ crystals were grown by the Bridgman method. High purity (6N) elemental Cd, Zn, and Te components were used. To provide a significant amount of Te inclusions, a Te excess ($\sim 5 \cdot 10^{18} \text{ cm}^{-3}$) was added specially to the stoichiometric composition of the solid solution. Wafers of ~ 15 mm were cut from

both ends of as-grown crystals for the preparation of control samples. Further, the crystals in the evacuated quartz container were inserted into the setup, in which a narrow zone heater was slowly moved along the container. The heater movement rate was 0.6 mm/day, and the temperature of hot zone was: $T = 780$ K (crystal No. 1) and $T = 870$ K (crystal No. 2).

Changes in the amount and morphology of Te inclusions before and after the MPHZ application were evaluated using infrared (IR) transmission microscopy. Since the matrix of $Cd_{0.9}Zn_{0.1}Te$ crystals is transparent for IR-wavelengths and Te inclusions are opaque, the IR-images show the shape, size and location of inclusions, as well as their distribution within the crystal. Images of crystal's bulk were obtained using a Leitz microscope, equipped with an infrared camera Pixelink PL-A741.

Electro-physical measurements were carried out on rectangular single-crystal samples ($12 \times 2 \times 1.5 \text{ mm}^3$) with two pairs of potential contacts in DC-mode and magnetic field of $B = 0.5$ T. Current contacts and two pairs of Hall contacts were created by the chemical deposition of copper from $CuSO_4$ solution followed by soldering of copper wires with In–Sn alloy. Signals were measured by an electrometer with input resistance of 10^{12} Ohm and sensitivity of 0.1 mV. Temperature dependences (TD) of specific conductivity σ and the Hall constant R_H , as well as the Hall mobility of current carriers $\mu = \sigma R_H$ were investigated in the temperature range of $90 \div 400$ K.

The transmission spectra of the samples before and after MPHZ were studied on an infrared spectrophotometer IRS-29 (wavelength range of $2.4 \div 25 \text{ }\mu\text{m}$) and on an automated setup based on the diffraction-lattice monochromator MDR-2 (wavelength range of $0.40 \div 0.95 \text{ }\mu\text{m}$).

3. Results and discussion

Comparison of IR-images of $Cd_{0.9}Zn_{0.1}Te$ samples before and after MPHZ (Fig. 1) shows the high efficiency of this method for these crystals: the density of inclusions in crystals was $\sim 10^6 \text{ cm}^{-3}$ before MPHZ, and $1 \div 10 \text{ cm}^{-3}$ after MPHZ.

Samples of $Cd_{0.9}Zn_{0.1}Te$ crystals before and after MPHZ are characterized by hole conductivity, and their resistivity before and after MPHZ was, respectively: 1.4 and 5.6 Ohm·cm (crystal No. 1), 25.4 and 27.4 Ohm·cm (crystal No. 2). Fig. 2 shows the

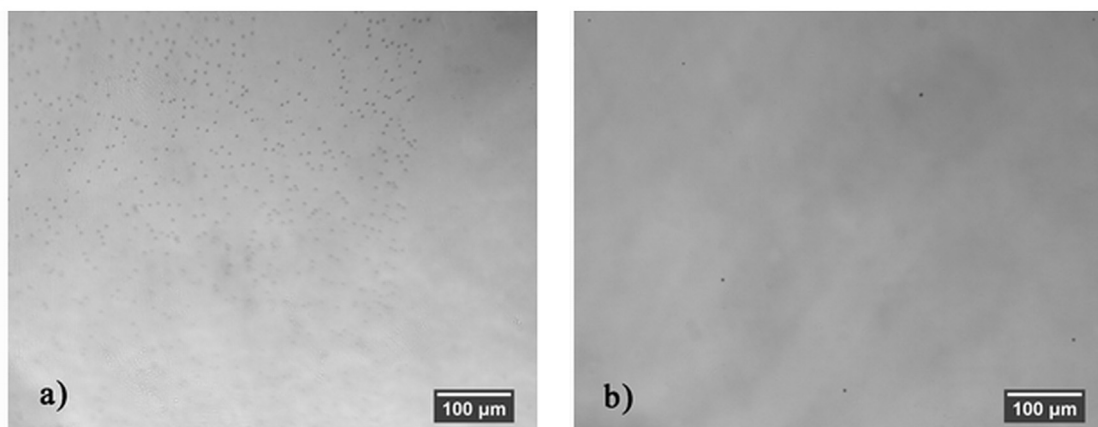


Fig. 1. Typical IR-images of Cd_{0.9}Zn_{0.1}Te crystal samples: before (a) and after (b) MPHZ

Hall constant TD of the samples. Based on these data, within the framework of a model of compensated acceptors [18–20], the type of acceptors controlling the *p*-conductivity was determined and their concentration was estimated. For calculations based on the experimental curves (Fig. 2), the following values were used: effective mass of holes $m_p = 0.63m_0$ [21], a statistical factor $\beta = 4$ for acceptors A_1 and $\beta = 2$ for acceptors A_2 [18]. It was determined that in sample 1 (curve 1), there are shallow acceptors A_1 ($E_A \approx 0.03$ eV) at $T \leq 160$ K and deeper acceptors A_2 ($E_A \approx 0.15$ eV) at higher temperatures. In other samples, only the acceptors A_2 exist, while the acceptors A_1 are fully compensated.

More complete information on the state of defect-impurity system in the studied samples was obtained from the TD analysis of hole mobility μ (Fig. 3). The influence of three mechanisms of current carrier scattering was taken into account: on crystal lattice vibrations (on optical phonons), on isolated ionized centers with concentration N_i , and on space-charge regions (SCRs) [22].

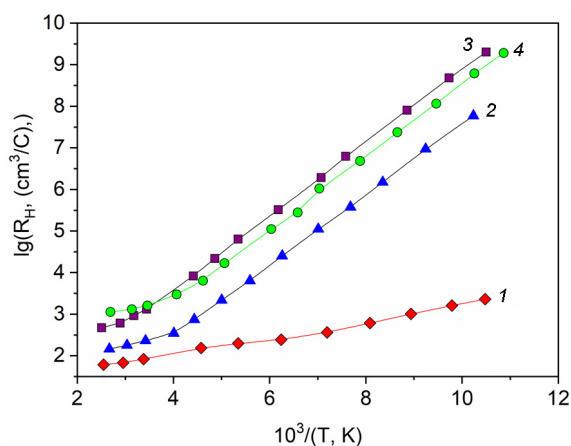


Fig. 2. Temperature dependences of the Hall constant R_H for Cd_{0.9}Zn_{0.1}Te samples: 1, 2 — crystal No. 1, before and after MPHZ; 3, 4 — crystal No. 2, before and after MPHZ, respectively.

acter of mobility TD at low temperatures (sample No. 1 in Fig. 3a and sample No. 2 in Fig. 3b).

The value of mobility μ_s , caused by scattering on the SCR was calculated by the

Table 1. Electro-physical characteristics of Cd_{0.9}Zn_{0.1}Te crystal samples before and after MPHZ

| No. of crystal | State of sample | T = 300 K | | N_i, cm^{-3} | $[A_1], \text{cm}^{-3}$ | $[A_2], \text{cm}^{-3}$ | $[D], \text{cm}^{-3}$ |
|----------------|-----------------|-----------------------------|--|-----------------------|-------------------------|-------------------------|-----------------------|
| | | $R_H, \text{cm}^3/\text{C}$ | $\mu_p, \text{cm}^2/(\text{V}\cdot\text{s})$ | | | | |
| 1 | before MPHZ | $1.0 \cdot 10^2$ | 73 | $3.0 \cdot 10^{17}$ | $1.8 \cdot 10^{17}$ | $5.5 \cdot 10^{16}$ | $1.6 \cdot 10^{17}$ |
| | after MPHZ | $2.8 \cdot 10^2$ | 50 | $4.5 \cdot 10^{16}$ | $0.9 \cdot 10^{16}$ | $4.6 \cdot 10^{16}$ | $2.3 \cdot 10^{16}$ |

The involvement of the third scattering mechanism is caused by the need to coordinate anomalous low values of mobility at high temperatures (at 300 K) with the char-

formula $\mu_s \sim (p_i)^{1/3} T^{-5/6}$, where p_i is the value of the screening charge (for low temperatures: $p_i = p_s$).

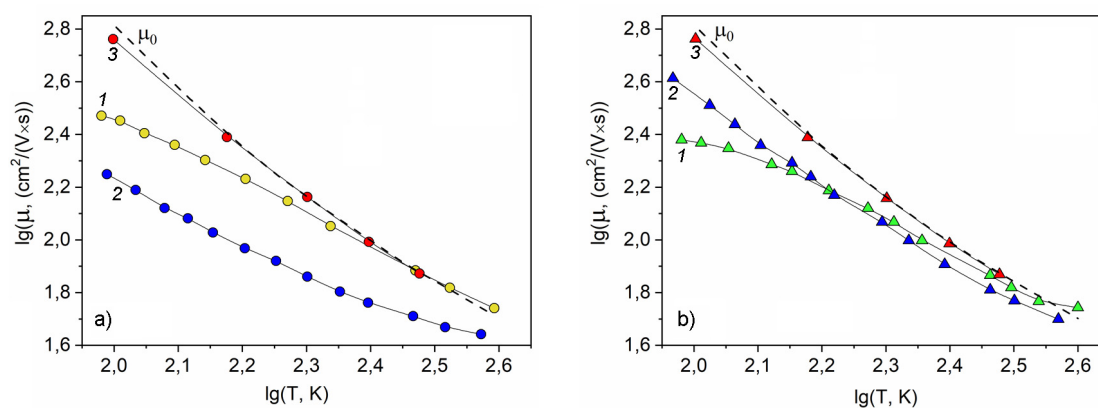


Fig. 3. Temperature dependences of hole mobility in $\text{Cd}_{0.9}\text{Zn}_{0.1}\text{Te}$ samples of crystal No. 1 (a), crystal No. 2 (b): 1 — before MPHZ, 2 — after MPHZ; 3 — calculated for sample after MPHZ by the exception of scattering on the SCR; μ_0 is limited by scattering on the lattice vibrations [18].

The μ_s was removed from the experimental values μ_{exp} by the Yamada rule [18]:

$$1/\mu = 1/\mu_{exp} - 1/\mu_s, \quad (1)$$

and TD of the mobility μ limited only by the first two scattering mechanisms was calculated (curve 3 in Fig. 3).

The overall purity of the crystals can be estimated by the total concentration of ionized scattering centers N_i . The N_i value was determined using the carrier mobility TD and the Brooks-Hering formula [18] for calculation of the mobility limited by scattering on ionized impurities. The concentration of shallow acceptors A_1 and compensating donors D was also evaluated (Table 1).

The effect of MPHZ is obvious: it provides a decrease in the order of concentration of ionizing centers in both crystals. This decrease was mainly due to the decrease in the concentration of shallow acceptors A_1 (and compensating donors), the concentration of deeper acceptors A_2 changed slightly.

In the absorption spectra obtained in the photon energy region of (0.05÷0.5) eV (Fig. 4), two regions can be noted: A — impurity absorption and B — absorption by free

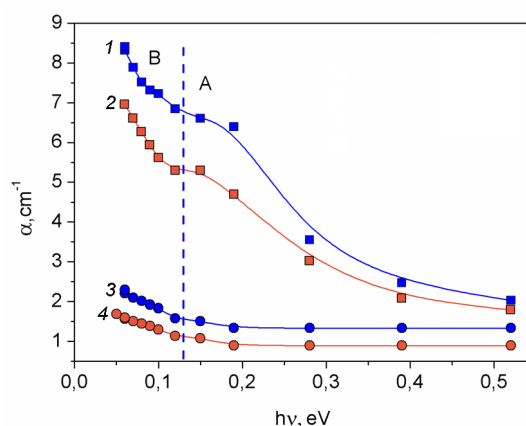


Fig. 4. Infrared absorption spectra (α_1 in Table 2) of $\text{Cd}_{0.9}\text{Zn}_{0.1}\text{Te}$ samples: 1, 2 — crystal No. 1 (before and after the MPHZ, respectively), 3, 4 — crystal No. 2 (before and after MPHZ, respectively).

carriers. It is difficult to separate these regions reliably, but it can be argued that the transition from region A to region B correlates well with the ionization energy of acceptors A_2 . The absorption of photons by these acceptors can be described by the reaction:

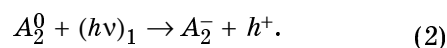


Table 2. Coefficients of impurity absorption and concentration of the corresponding acceptors in $\text{Cd}_{0.9}\text{Zn}_{0.1}\text{Te}$ crystal samples

| No. of crystal | State of sample | $[A_2], \text{cm}^{-3}$ | α_1, cm^{-1} | $(0.15 \text{ eV}) [A_1], \text{cm}^{-3}$ | α_2, cm^{-1} (1.55 eV) |
|----------------|-----------------|--------------------------|----------------------------|---|---|
| 1 | before MPHZ | $\sim 5.5 \cdot 10^{16}$ | 6.61 | $1.8 \cdot 10^{17}$ | — |
| | after MPHZ | $4.6 \cdot 10^{16}$ | 5.30 | $0.9 \cdot 10^{16}$ | — |
| 2 | before MPHZ | $1.6 \cdot 10^{16}$ | 1.51 | $3.3 \cdot 10^{16}$ | 42 |
| | after MPHZ | $1.2 \cdot 10^{16}$ | 1.08 | $0.3 \cdot 10^{16}$ | 30 |

Table 3. Comparison of the electro-physical characteristics of CdTe [16], Cd_{0.95}Mn_{0.05}Te [17] and Cd_{0.9}Zn_{0.1}Te crystals before and after MPHZ

| Crystal | before MPHZ | after MPHZ | | | | |
|--|------------------------|-------------------|-----------------------|-------------------------|-------------------------|-----------------------|
| | N_i, cm^{-3} | Conductivity type | N_i, cm^{-3} | $[A_1], \text{cm}^{-3}$ | $[A_2], \text{cm}^{-3}$ | $[D], \text{cm}^{-3}$ |
| CdTe | $\sim 3 \cdot 10^{17}$ | n | $1.0 \cdot 10^{16}$ | $0.5 \cdot 10^{16}$ | | $0.5 \cdot 10^{16}$ |
| Cd _{0.95} Mn _{0.05} Te | $\sim 3 \cdot 10^{17}$ | p | $9.0 \cdot 10^{16}$ | $2.3 \cdot 10^{16}$ | $2.7 \cdot 10^{16}$ | $4.5 \cdot 10^{16}$ |

In this regard, the results of optical and electrical measurements can be compared: the value of impurity absorption coefficient α_1 with the calculated concentrations of acceptors A_2^0 in samples before and after MPHZ (Table 2). It can be seen that an increase of heater temperature in the MPHZ process from 780 K to 870 K did not affect the purification quality.

As to shallow acceptors A_1 , they are also involved in the light absorption processes, but no good correlation between the optical and electrical data, as in the case of acceptors A_2 , has been found for them. The spectral dependences in an intrinsic absorption region (Fig. 5) confirm the improvement in the optical transmission in crystals after MPHZ.

MPHZ was previously used for the purification of undoped CdTe crystals [16] and for Cd_{0.95}Mn_{0.05}Te crystals [17], so it will be useful to compare the results, obtained in this paper for Cd_{0.9}Zn_{0.1}Te with the results presented in the mentioned works. Analysis of the data, summarized in Table 3, shows that MPHZ has the greatest influence on the purification of undoped CdTe crystals: tellurium inclusions was practically absent, the crystals conductivity changed from p - to n -type, and the concentration of ionized centers decreased by more than an order of magnitude, the carrier mobility increased from $61 \text{ cm}^2/(\text{V}\cdot\text{s})$ to $920 \text{ cm}^2/(\text{V}\cdot\text{s})$, and conductivity began to be controlled by the shallow donors ($E_D < 0.02 \text{ eV}$) [16]. The Te inclusions were also effectively eliminated in the case for Cd_{0.95}Mn_{0.05}Te crystals, however, the p -type conductivity remained, and concentration of ionized centers was reduced only by ~ 3.5 times [17]. Cd_{0.9}Zn_{0.1}Te crystals occupy an intermediate position in the MPHZ efficiency, although the conductivity type of the crystals has not changed, but concentration of ionized centers decreased by ~ 6.5 times.

Since the technological parameters in the purification process of all three crystals remained the same, it is very probably that

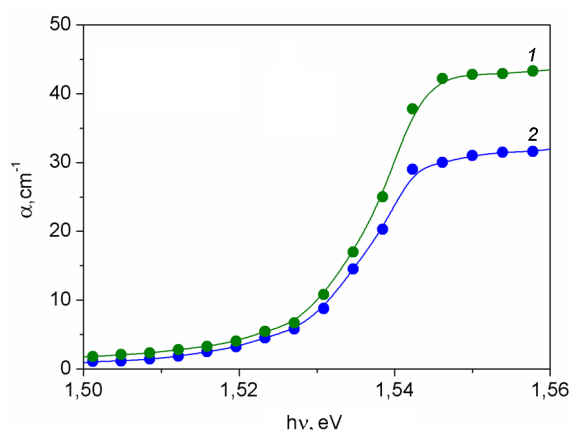


Fig. 5. Spectral dependences of the absorption coefficient in Cd_{0.9}Zn_{0.1}Te samples of crystal No. 2: 1, 2 — before and after MPHZ, respectively.

the presence of additional impurities in Mn or Zn components is affected the MPHZ efficiency. Because Mn is more dirty (4N-5N) than Zn, it can be the source of a large amount of uncontrolled impurities in the crystal, the concentration of which is difficult to significantly reduce using MPHZ.

4. Conclusions

The application of the hot zone purification method (zone temperatures of 780 K, 870 K, the zone speed 0.6 mm/day) to the Cd_{0.9}Zn_{0.1}Te crystals effectively eliminates the Te inclusions; this improves the crystal-line quality and optical transparency. It is ensured that the crystal is free from uncontrolled impurities that dissolve in molten tellurium, namely:

- the concentration of shallow acceptors A_1 reduces by an order of magnitude ($\epsilon_A = 0.03 \text{ eV}$), which leads to the reduction of light absorption coefficient near the edge of the fundamental band;
- the concentration of acceptors A_2 ($\epsilon_A = 0.15 \text{ eV}$) reduces, which leads to the reduction of light absorption coefficient in

the infrared region of the spectrum ($0.15 \div 0.35$) eV.

Taken together, these effects lead to the reduction in the concentration of ionized centers by almost an order of magnitude, that is, to an increase of the material purity.

References

1. R.Triboulet, P.Siffert, European Materials Research Society series, Elsevier, Oxford (2010).
2. U.N.Roy, A.Burger, R.B.James, *J. Cryst. Growth*, **379**, 57 (2013).
3. Ya-dong Xu, Wan-qi Jie, Yi-hui He et al., *Pro. Nat. Sci-Mater.*, **21**, 66 (2011).
4. Xiao-yan Liang, Jia-hua Min, Liu-qing Yang et al., *Mater. Sci. Semicond. Process.*, **40**, 939 (2015).
5. M.Shkir, V.Ganesh, S.AlFaify et al., *Cryst. Growth & Design.*, **18**, 2046 (2018).
6. J.H.Greenberg, V.N.Guskov, *J. Cryst. Growth*, **289**, 552 (2006).
7. Y.Gu, C.Rong, Y.Xu et al., *Nucl. Instr. Meth. Phys. Res. B*, **343**, 89 (2015).
8. R.Guo, W.Jie, Y.Xu et al., *Nucl. Instr. Meth. Phys. Res. A*, **794**, 62 (2015).
9. Y.Gua, W.Jie, L.Li et al., *Micron*, **88**, 48 (2016).
10. K.H.Kim, J.Suh, A.E.Bolotnikov et al., *J. Cryst. Growth*, **354**, 62 (2012).
11. G.Yang, A.E.Bolotnikov, P.M.Fochuk et al., *J. Cryst. Growth*, **379**, 16 (2013).
12. P.Fochuk, R.Grill, O.Kopach et al., *IEEE Trans. Nucl. Sci.*, **59**, 256 (2012).
13. C.Xu, F.Sheng, J.Yang., *J. Cryst. Growth*, **451**, 126 (2016).
14. E.Kim, Y.Kim, A.E.Bolotnikov et al., *Nucl. Instr. Meth. Phys. Res. A*, **923**, 51 (2019).
15. G.Piacentini, N.Zambelli, G.Benassi et al., *J. Cryst. Growth*, **415**, 15 (2015).
16. P.Fochuk, Z.Zakharuk, Ye.Nykonyuk et al., *IEEE Trans. Nucl. Sci.*, **63**, 1839 (2016).
17. Z.Zakharuk, S.Dremlyuzhenko, S.Solodin et al., *J. Nano-Electron. Phys.*, **9**, 06004-1 (2017).
18. K.Zanio, Semiconductors and Semimetals, Academic Press, New York, (1978).
19. L.A.Kosyachenko, Z.I.Zakharuk, A.V.Markov et al., *Ukr. J. Phys.*, **49**, 573 (2004).
20. Y.S.Nykoniuk, Z.I.Zakharuk, E.V.Rybak et al., *Semicond.*, **40**, 781 (2006).
21. P.Ravindran, Carrier Effective Mass Calculations, Computational Condensed Matter Physics, Springer (2015).
22. P.Fochuk, Ye.Nykoniuk, Z.Zakharuk et al., *IEEE Trans. Nucl. Sci.*, **64**, 2725 (2017).